Dyes and Pigments 94 (2012) 127–135

Contents lists available at SciVerse ScienceDirect

Dyes and Pigments

journal homepage: www.elsevier.com/locate/dyepig

Synthesis of novel DNA-interacting phthalocyanines

Canan Uslan, B. Şebnem Sesalan*

Istanbul Technical University, Faculty of Science and Letters, Department of Chemistry, Maslak 34469, Istanbul, Turkey

ARTICLE INFO

Article history:
Received 13 October 2011
Received in revised form
21 November 2011
Accepted 3 December 2011
Available online 14 December 2011

Keywords:
Metallophthalocyanine
DNA
Singlet oxygen
Quaternization
Gel electrophoresis
Photosensitizer

ABSTRACT

The new copper hexamethyleneimino-ethoxy substituted phthalocyanine (pc) (**2**) and its quaternized derivative (**2Q**) were synthesized. The interaction of quaternized copper (**2Q**), quaternized cobalt (**3Q**) and zinc (**4Q**) phthalocyanines (pcs) with calf thymus (CT) DNA was investigated by UV/Vis spectrophotometric methods and gel electrophoresis. With the addition of pcs, the change in the thermal denaturation profile of DNA was observed. The results indicated that these molecules exhibit efficient DNA binding activity. Generation of singlet oxygen by **2** and **2Q** and photocleavage of CT-DNA were determined. All the experimental data proved that these water soluble pcs can act as active components in the photocleavage of DNA.

1. Introduction

Design and development of nucleic acid targeting drugs are very powerful means in the search for new potent drugs. Although many synthetic compounds have been developed to explore a variety of DNA/RNA structures, few molecules can be used to photocleave DNA in the concept of photodynamic therapy (PDT) [1]. The interaction and reaction of metal complexes with DNA have long been the subject of intense investigation in relation to the development of new reagents for biotechnology and medicine [2]. Metal compounds have also been used as antitumor agents due to cytotoxic effects of metals [3,4].

Since they possess a great planar area and extended π system, pcs are one of the largest classes of macromolecules which can be modified easily according to target. The properties that make pc dyes particularly attractive as potential bioassay reagents include their high molar absorptivity, resistance to chemical and photochemical degradation, absorption and emission in the deep red region of the electromagnetic spectrum, long lifetimes with high quantum yields [5–7]. A particularly attractive feature of pcs is the possibility of tuning its electrical, optical, catalytic and photochemical properties through slight changes on the nature of the peripheral substituents or using different central metal ions in the pc core [8,9].

Pcs can coordinate a variety of metals in their central cavity, which further enables tailoring their spectral and photophysical properties because the metal can affect the pathways of the excited MPc returning to the ground state, in particular the rate of intersystem crossing resulting from metal–ligand spin-orbit coupling [10,11].

In order to overcome the insolubility of unsubstituted pc parent molecule, peripheral groups have been extensively used to enhance solubility [12–14]. Water soluble pcs have appeared as attractive compounds for biomedical applications.It is known that cationic pcs form complexes with nucleic acids [15–20]. The binding of positively charged oligonucleotide substituted pcs with single- and double-stranded DNA was investigated. It was shown that these pcs interact with nucleic acids through an outside binding mode [21].

On the other hand, several pc systems such as the zinc pcs or silicon (IV) pcs have also been introduced for PDT in research and clinical trials [22]. Due to their high molar absorption coefficient in the red part of the spectrum, photostability and long lifetimes of the photoexicited triplet states, pcs are known to be useful photosensitizers [23–25].

Our group have been engaged with the synthesis of phthalocyanines and porphyrazines with different functional moieties serving for many different purposes. Among the many, we may cite the substituents which include heterocyclic groups, porphyrazine–phthalocyanine hybrid units and quaternized amino groups [26–32]. The use of an inactive precursor is an important strategy

* Corresponding author. Tel.: +90 212 285 33 03; fax: +90 212 285 63 86.
E-mail address: sungurs@itu.edu.tr (B. Şebnem Sesalan).

0143-7208/$ – see front matter © 2011 Elsevier Ltd. All rights reserved.
doi:10.1016/j.dyepig.2011.12.003

in drug targeting [33]. In this perspective, we decided to study with copper, cobalt and zinc incorporated pcs which have the potential use for cancer treatment.

Among the different pcs employed for DNA binding studies, the positively charged pcs are the most efficient ones in terms of binding and cleaving DNA as compared with either the neutral or negatively charged pcs. In this context, our previous photochemical studies on the hexamethyleneimino substituted pcs [10] lead us to examine the interaction of copper (**2Q**), cobalt (**3Q**) and zinc (**4Q**) MPcs with CT-DNA. To clarify the binding mode of MPcs (Fig. 1) to CT-DNA, UV/Vis-titration experiments, DNA gel electrophoresis were performed and the changes in CT-DNA thermal denaturation profiles were determined. Afterward, we experienced the photo-induced DNA cleaving abilities of these macrocycles.

2. Experimental

2.1. Materials

All reagents and solvents were of reagent grade quality and were obtained from commercial suppliers. N-(2-hydroxyethyl) hexamethyleneimine was purchased from Aldrich.1,3-diphenylisobenzofuran (DPBF) and 9,10-Antracenediyl-bis(methylene)dimalonoic acid (ADMA) were purchased from Fluka. All solvents were dried and purified as described by Perrin and Armarego [34]. 4-Nitrophthalonitrile was synthesized according to [35]. The compounds **1**, **3**, **4**, **3Q** and **4Q** were prepared with similar methods prior to previous work [10].

2.2. Equipment

^{1}H NMR spectra were recorded on a Varian Mercury 200 MHz spectrometer in $CDCl_3$ and DMSO-d_6. Chemical shifts were reported (δ) relative to Me_4Si as internal standard. Mass spectra were measured on a Micromass Quatro LC/ULTIMA LC–MS/MS spectrometer.

IR spectra were recorded on a Perkin–Elmer Spectrum One FT-IR spectrophotometer and electronic spectra on Scinco Neosys 2000 double beam UV/Vis Spectrophotometer with 1 cm path length quartz cuvettes in the spectral range of 300–800 nm. Elemental analysis and mass spectra were performed by the Instrumental Analysis Laboratory of TUBITAK. Melting temperature study was carried out using a thermostated Shimadzu-1901 UV/Vis spectrophotometer. All reagents and solvents were of reagent grade quality obtained from commercial suppliers.

Photo-irradiations were done using a General Electric quartz line lamp (300 W). A 600 nm glass cut off filter (Schott) and a water filter were used to filter off ultraviolet and infrared radiations, respectively. An interference filter (Intor, 670 nm with a band width of 40 nm) was additionally placed in the light path before the sample. Light intensities were measured with a THORLABS power meter.

Photocleavage of pBR322 was performed with 600–700 nm diode laser. The products were run by gel electrophoresis on 1% agarose gel in phosphate buffer solution (pH 7.4), stained with SYBR Green I and analyzed photographically under UV illumination.

2.3. Synthesis

2.3.1. Synthesis of 2,9(10),16(17),23(24)-tetrakis-(2-hexamethylenimino-ethanoxy) phthalocyaninato copper (II) (2)

Anydrous copper (II) chloride (0.024g, 0185 mmol) was dissolved in dry n-pentanol (5 mL) and 1 (0.1 g, 0.37 mmol) were refluxed in the presence of DBU (3 drops) under nitrogen. After 24h, 15 mL of acetone was added to the mixture and centrifuged (4000 × *g*) for 3 min. The precipitate was filtered and washed with acetone till the filtrate was colorless. The crude product was dissolved in 5 mL THF and added dropwise into 20 mL of cold hexane. The precipitate was filtrated and washed with hexane (10 mL × 5) and dried under vacuum. Yield: 52.92 mg, (49.97%). (Found: C, 67.41; H, 7.09; N, 13.98%. (1140.91) $C_{64}H_{76}CuN_{12}O_4$ requires C, 67.37; H, 6.71; N, 14.73%). IR ν_{max}/cm^{-1}: 2917, 2949 (Aliph C–H), 1645, 1522, 1456, 1405 (Arom–C–H), 1339, 1235, 1120-1061 (C–O–C), 850, 820,750. MS [*m*/*z*]: 1140.95 $[M]^+$. UV/Vis λ_{max} (nm) DMF: 682 (4.58), 625 (4.36), 336 (4.51).

2.3.2. Synthesis of quaternized 2,9(10),16(17),23(24)-tetrakis-(2-hexamethylenimino-ethanoxy)phthalocyaninato copper (II) (2Q)

These complexes were prepared according to the method previously reported [36]. Compound 2 (70 mg, 0.061 mmol) was heated to 120 °C in freshly distilled DMF (5 mL) and excess dimethyl sulfate (0.1 mL) was added dropwise. The mixture was stirred at 120 °C for 12 h. After this time, the mixture was cooled to room temperature and the product was precipitated with hot acetone and collected by filtration. The blue solid product was washed successively with hot ethanol, ethyl acetate, THF, chloroform, n-hexane and diethylether. The resulting hygroscopic product was dried over phosphorous pentoxide. Yield: 42.5 mg, % 49.6. IR $\nu_{max}/(cm^{-1})$: 2928; 2858; 1599; 1506; 1456; 1402; 1342; 1286; 1227; 1189; 1134; 1093; 1004; 956; 821; 745. MS [*m*/*z*]: 1394.95 $[M]^+$. Found: C, 58.52; H, 6.29; N, 12.15%. $C_{68}H_{88}CuN_{12}O_{12}S_2$ requires C, 58.62; H, 6.37; N, 12.06%.

2.4. Singlet oxygen quantum yields

Singlet oxygen quantum yield (Φ_Δ) determinations were carried out using the experimental set-up described in literature [37,38]. Typically, a 3 cm^3 portion of the respective substituted copper (**2**) (Fig. 2) and **2Q** (Figs. 3 and 4b) phthalocyanine derivatives, (concentration = 1×10^{-5} M) containing the singlet oxygen quencher was irradiated in the Q band region with the photo-irradiation set-up described in references [37,38]. Singlet oxygen quantum yields (Φ_Δ) were determined in air using the relative method with unsubstituted ZnPc (in DMSO) or $ZnPcS_{mix}$ (in aqueous media) as references. DPBF and ADMA were used as chemical quenchers for singlet oxygen in DMSO and aqueous media, respectively. Eq. (1) was employed for the calculations:

$$\Phi_\Delta = \Phi_\Delta^{Std} \frac{R I_{abs}^{Std}}{R^{Std} I_{abs}} \quad (1)$$

where Φ_Δ^{Std} is the singlet oxygen quantum yields for the standard unsubstituted ZnPc ($\Phi_\Delta^{Std} = 0.67$ in DMSO) [39] and $ZnPcS_{mix}$ ($\Phi_\Delta^{Std} = 0.45$ in aqueous media) [40]. R and R_{Std} are the DPBF (or ADMA) photobleaching rates in the presence of the phthalocyanine derivatives and standards, respectively. I_{abs} and I_{abs}^{Std} are the rates of light absorption by phthalocyanine derivatives and standards, respectively. To avoid chain reactions induced by DPBF (or ADMA) in the presence of singlet oxygen [41], the concentration of quenchers (DPBF or ADMA) was lowered to $\sim 3 \times 10^{-5}$ M. Solutions of sensitizer containing DPBF (or ADMA) were prepared in the dark and irradiated in the Q band region using the set-up described above. DPBF degradation at 417 nm (in DMSO) and ADMA degradation at 380 nm (in water) were monitored. Singlet oxygen quantum yields of **2**, **2Q**, **3** [10], **4** [10], **3Q** [10] and **4Q** [10] were given in Table 1. Singlet oxygen quantum yields are the arithmetic average of 5 experiments with the average standard deviations of 0.20 in DMSO and 0.21 in water for **2Q** (Table 1).

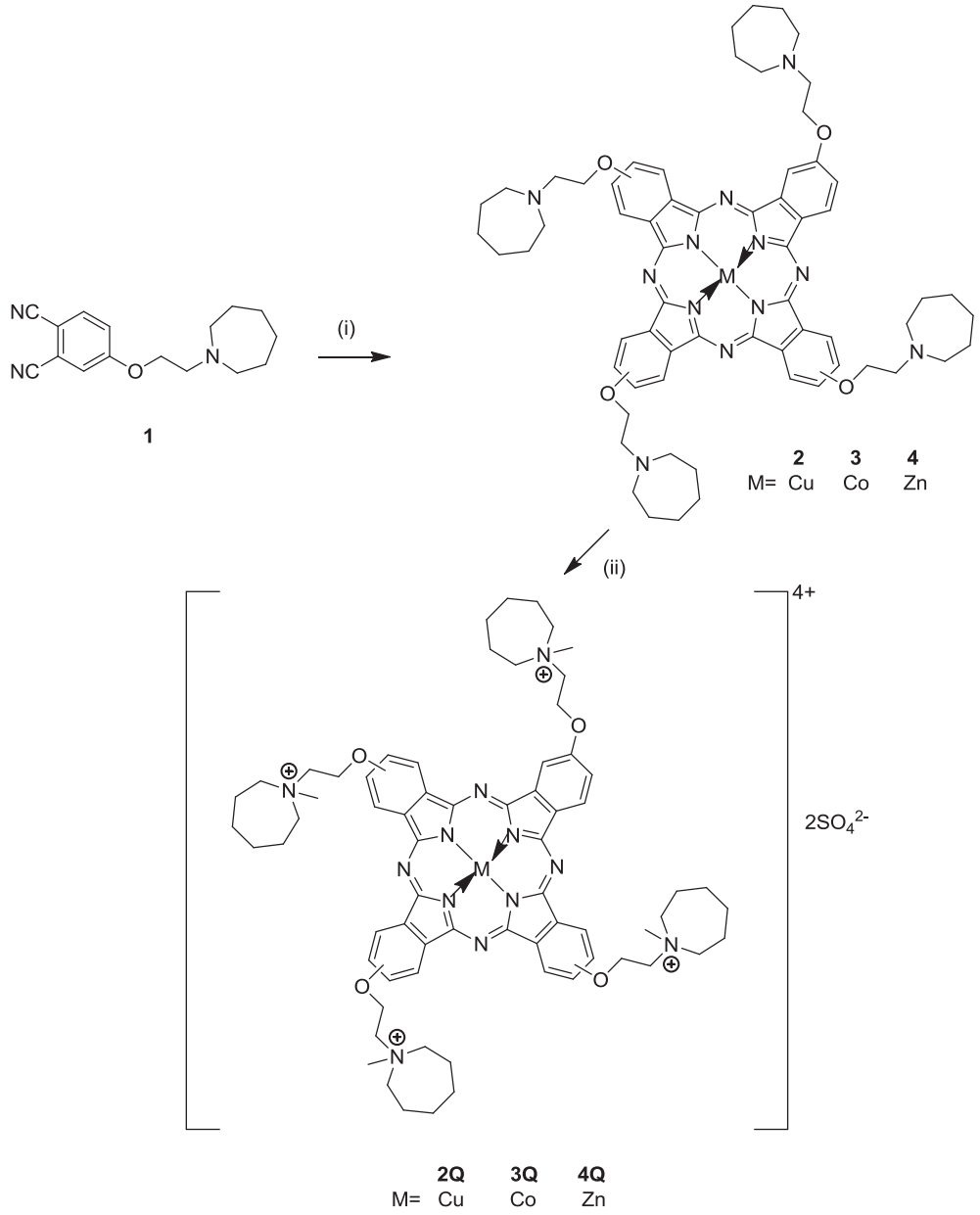

Fig. 1. The synthesis of new metallophthalocyanines (MPcs). For the synthesis of **2** i) Anhydrous copper (II) chloride, dry n-pentanol, reflux, DBU, 24 h, N_2 [10] ii) [10].

2.5. Binding studies of quaternized zinc and cobalt phthalocyanine complexes to DNA

2.5.1. Determination of binding of 2Q, 3Q and 4Q to DNA using UV/Vis titrations

All titrations of pcs with CT-DNA were performed at room temperature in phosphate buffer (pH 7.40). The concentrations of CT-DNA per nucleotide phosphate ([DNA]) were calculated from the absorbance at 260 nm using DNA = 6600 $M^{-1}cm^{-1}$ [42]. CT-DNA was stored at 4 °C overnight and used within 2 days. Absorption spectra were collected from 300 nm to 800 nm. The titrations were carried out until MPcs' Q bands remained at a fixed wavelength upon successive additions of CT-DNA. 10 successive injections (each contained 5 μL 0.62 mM CT-DNA) were added manually to 0.035 mM, 1.5 mL buffer solution of **2Q**, **3Q** or **4Q**. The decrease in absorbance continued until a stable dye–Pc complex formed. After 25 μL (5 × 5 μL) 0.62 mM CT-DNA addition to ***2Q*** and ***3Q***, negative and positive charge neutralization between DNA and dye occurred (Figs. 5 and 6). However, 35 μL (7 × 5 μL) 0.62 mM CT-DNA required for a stable dye–pc complex formation in case of ***4Q*** (Fig. 7). The binding constant K_a was determined by [42] given in Eq. (2):

$$C/\Delta\varepsilon_a = C/\Delta\varepsilon_a + 1/(\Delta\varepsilon K_a) \quad (2)$$

C is the concentration of DNA, $\Delta\varepsilon_a = [\varepsilon_a - \varepsilon_f]$, $\Delta\varepsilon = [\varepsilon_b - \varepsilon_f]$, and ε_a, ε_b and ε_f correspond to the apparent extinction coefficient of **2Q**, **3Q** or **4Q**, the extinction coefficient of the bound form of **2Q**, **3Q** or **4Q** and that of free of **2Q**, **3Q** or **4Q**, respectively.

2.5.2. Determination of the change in thermal denaturation profile of DNA

Melting temperatures were determined for CT-DNA (0.62 mM, 0.9 mL) and ***2Q***, ***3Q*** or ***4Q*** (0.065 mM, 0.1 mL) in buffer (pH 7.4) by

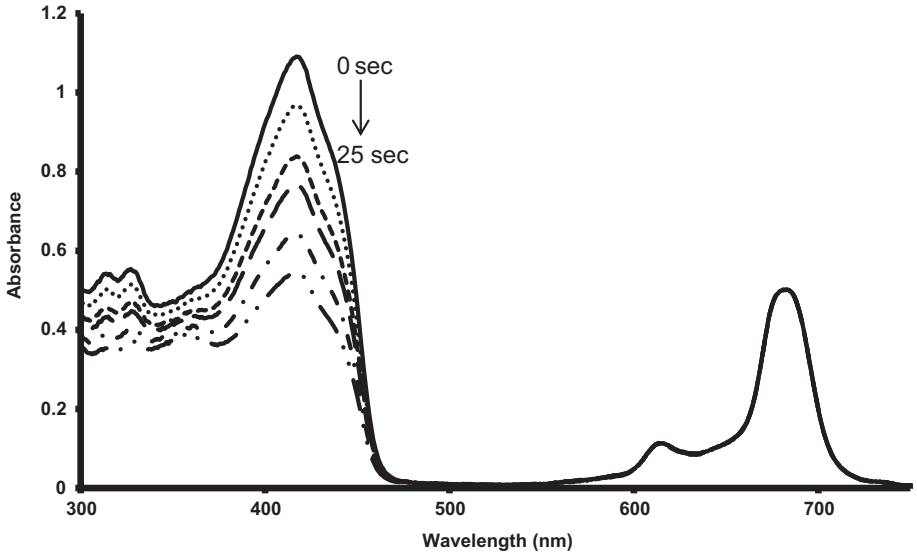

Fig. 2. Electronic spectrum of photodegradation of DPBF in DMSO indicating the singlet oxygen generation by complex **2** (1×10^{-5} M). The more the intensity of the absorbance at 415 nm decrease, the more singlet oxygen produced.

heating from 25 to 90 °C at a rate of 0.6 °C/min, recording the UV absorbance at 260 nm every 10 s (Fig. 8). The absorbances were the means of 5 repeats. The average standard deviations were of 0.22, 0.20 and 0.17 for ***2Q***, ***3Q*** and ***4Q*** respectively.

2.5.3. Determination of binding 2Q, 3Q and 4Q to DNA using gel electrophoresis

36 μM DNA (dissolved in 1 mL PBS), **2Q**, **3Q** and **4Q** solutions were used. R refers to the ratio of [MPc]/[DNA] indicated in Table 2. The products were run by gel electrophoresis on 1% agarose gel in phosphate buffer solution (pH 7.4), stained with SYBR Green I and analyzed photographically under UV illumination (Fig. 9). Migration conditions were optimized to 20 min and 120V. 5 μL loading dye and 5 μL DNA was loaded then MPcs were loaded in wells with different R values.

2.6. Determination of photocleavage of plasmid DNA using gel electrophoresis

The experiments were performed in 0.5 mL plastic eppendorf microcentrifuge tubes. Each tube contained 10 μL (0.2 μg) of supercoiled DNA (pBR322) and 5 μM **2Q**, **3Q** and **4Q** solutions were prepared in phosphate buffer (pH = 7.4). Tubes were illuminated from top and in air at room temperature with 600–700 nm diode laser which was placed 5 cm away from the tested tubes. Irradiation time changed from 1 to 5 min without changing the concentrations of the reactants in each tube. After irradiation, conversion of supercoiled DNA (form I) to nicked circular DNA (form II) was visualized by agarose gel electrophoresis and subsequent SYBR Green I staining. Results of DNA cleavage by **2Q**, **3Q** and **4Q** were illustrated in Fig. 10.

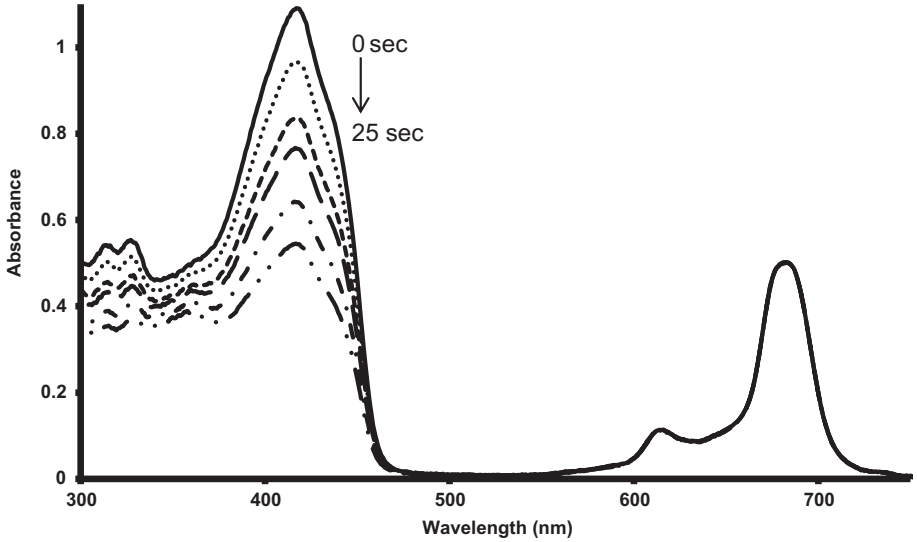

Fig. 3. Electronic spectrum of photodegradation of DPBF in DMSO indicating the singlet oxygen generation by complex **2Q** (1×10^{-5} M). The more the intensity of the absorbance at 415 nm decrease, the more singlet oxygen produced.

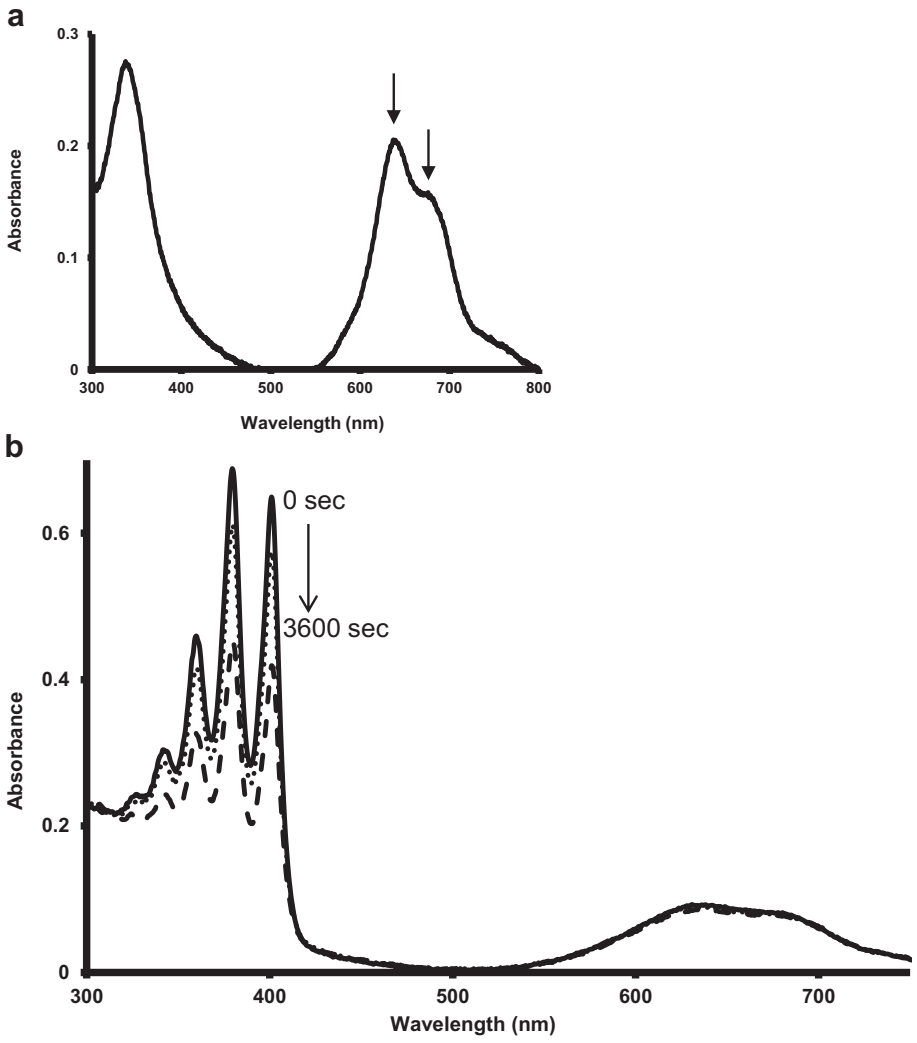

Fig. 4. Electronic absorption spectrum of (a) **2Q** in buffer; (b) photodegradation of ADMA in buffer (pH = 7.4) indicating the singlet oxygen generation by complex **2Q** (1×10^{-5} M). The more the intensity of the absorbance at 380 nm decrease, the more singlet oxygen produced.

3. Results and discussion

3.1. Synthesis and characterization

The synthesis and characterization of the compounds **1**, **3**, **3Q**, **4** and **4Q** were given in the previous work [10]. The synthetic procedure of the phthalocyanine complexes **2** and **2Q** was given in Fig. 1. The new copper pc was prepared according to the similar previous method [10]. Briefly, (2-hexamethylenimino-ethoxy) substituted phthalonitrile derivative (**1**) was synthesized through base-catalyzed aromatic displacement of 4-nitrophthalonitrile with N-(2-hydroxyethyl) hexamethyleneimine using K_2CO_3 as the base in dry DMF. The reactions were carried out at 50 °C under N_2 atmosphere for 48 h. Cyclotetramerization of the phthalonitrile derivative (**1**) to the tetra-substituted copper pc was accomplished in the presence of anhydrous copper (II) chloride in dry n-penthanol and the crude product was purified column chromatography using alumina filled column. Quaternized copper pc (**2Q**) was obtained from the reaction of corresponding phthalocyanine (**2**) with excess of dimethyl sulfate in DMF for 12h in order to reach complete quaternization [36]. The structures of the target compounds were confirmed using IR, mass spectra and elemental analysis.

Table 1
Spectral data and singlet oxygen quantum yields (Φ_Δ) for copper (**2Q**), cobalt (**3Q**) and zinc (**4Q**) phthalocyanines in DMSO and water.

Compound	Solvent	**Q** band λ_{max}, (nm)	log ε	Φ_Δ
2Q[b]	DMSO	667	4.50	0.010[b]
	H_2O	625,668	4.21, 4.14	0.80[b]
3Q[a]	DMSO	668	4.53	0.012[a]
	H_2O	627, 669	4.22, 4.15	0.84[a]
4Q[a]	DMSO	683	4.77	0.36[a]
	H_2O	639, 678	4.30, 4.19	0.26[a]

[a] Detailed experimental data for **3Q** and **4Q** was given previously [10].
[b] Average standard deviations for singlet oxygen quantum yields of **2Q** in DMSO and in H_2O are 0.20 and 0.21 respectively.

For **2** and **2Q** the elemental analyses results are consistent with the expected ones. Cyclotetramerization of the dinitrile derivative (**1**) to copper (II) pc (**2**) was confirmed by the disappearance of the sharp C≡N vibration of 2229 cm^{-1} which was attributed to **1** [10]. The mass spectrum of **2** showed molecular ion peaks at $m/z = 1140.95$ $[M]^+$ supporting the proposed formula for the compound. Quaternized copper pc (**2Q**) was soluble in water, DMF and DMSO. No major change in the IR spectra was found after quaternization. Molecular mass of **2Q** was calculated as 1393.18 g. The mass spectra of quaternized copper pc (**2Q**)

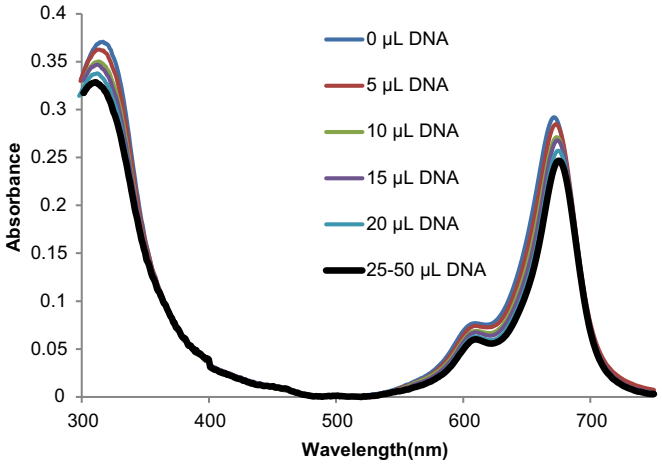

Fig. 5. Electronic spectrum of **2Q** upon increasing amounts of CT-DNA. 10 Successive injections (each contained 5 µL 0. 62 mM CT-DNA) were added to 0.035 mM, 1.5 mL buffer solution of **2Q**. Line 1: spectrum of the solution which contained 0.035 mM, 1.5 mL of **2Q**. Line 2–6: The decrease in absorbance continued (Line 2 (5 µL) to line 6 (25 µL)) until a stable dye–Pc complex formed. Line 7 (30 µL)–Line 11 (50 µL) (bold black lines): A stable dye–Pc complex formed when 25 µL (5 × 5) 0.62 mM CT-DNA was added to **2Q**; **Q** band absorbance remained constant after 5th addition.

confirmed the proposed structure, with the molecular ion being easily identified at 1394.95 $[M]^+$.

3.2. Singlet oxygen quantum yields

The singlet oxygen quantum yields (Φ_Δ), indicates the potential of the complexes as photosensitizers in PDT applications where singlet oxygen is required. The Φ_Δ values were determined using a chemical method (using DPBF in DMSO and ADMA in water as quenchers). The production of $^1O_2$ by **2** and **2Q** was determined indirectly by monitoring the decomposition of DPBF and ADMA. Fig. 2 showed the decrease in the absorbance intensity of DPBF in DMSO for complex **2**. The singlet oxygen generated by complex **2Q** was indicated as the disappearance of the absorbances of ADMA (Fig. 3) at 380 nm and DPBF (Fig. 4b) at 415 nm. There was no decrease in the Q band of formation of the studied phthalocyanine complexes during Φ_Δ determinations (Figs. 2–4b).

In water, quaternized complex **2Q** showed cofacial aggregation, and was proved by the presence of two non-vibrational peaks in the Q band region (Table 1). The lower energy (red-shifted) band at 668 nm for **2Q** is due to the monomeric specie, while the higher energy (blue-shifted) band at 625 nm for **2Q** is due to aggregated specie (Fig. 4a). The same case was also discussed for **3Q** and **4Q** [10]. Aggregation is usually depicted as a coplanar association of rings progressing from monomer to dimer and higher order complexes. It is dependent on the concentration, nature of the solvent, nature of the substituents, complexed metal ions and temperature [43].

The Φ_Δ value of quaternized ionic zinc phthalocyanine complex (**4Q**) is higher in DMSO than in water. However, the Φ_Δ value of quaternized ionic cobalt phthalocyanine complex (**3Q**) is the highest among the others in water than in DMSO. The Φ_Δ value of quaternized ionic copper phthalocyanine (**2Q**) complex is higher than **4Q** but less then **3Q**. Many factors are responsible for the magnitude of the determined quantum yield of singlet oxygen

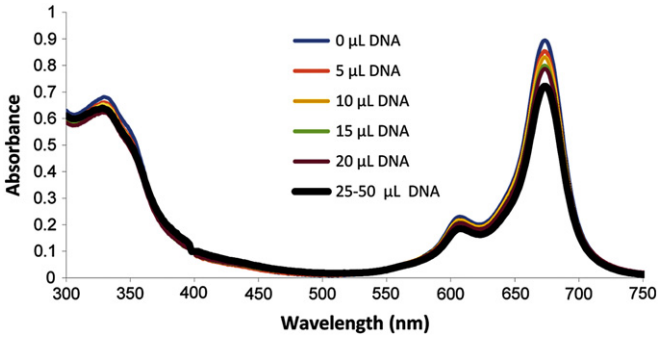

Fig. 6. Electronic spectrum of **3Q** upon increasing amounts of CT-DNA. 10 succesive injections (each contained 5 µL 0. 62 mM CT-DNA) were added to 0.035 mM, 1.5 mL buffer solution of **3Q**. Line 1: spectrum of the solution which contained 0.035 mM, 1.5 mL of **3Q**. Line 2–6: The decrease in absorbance continued (Line 2 (5 µL) to line 6 (25 µL)) until a stable dye–Pc complex formed. Line 7 (30 µL)–Line 11 (50 µL) (bold black lines): A stable dye–Pc complex formed when 25 µL (5 × 5) 0.62 mM CT-DNA was added to **3Q**; **Q** band absorbance remained constant after 5th addition.

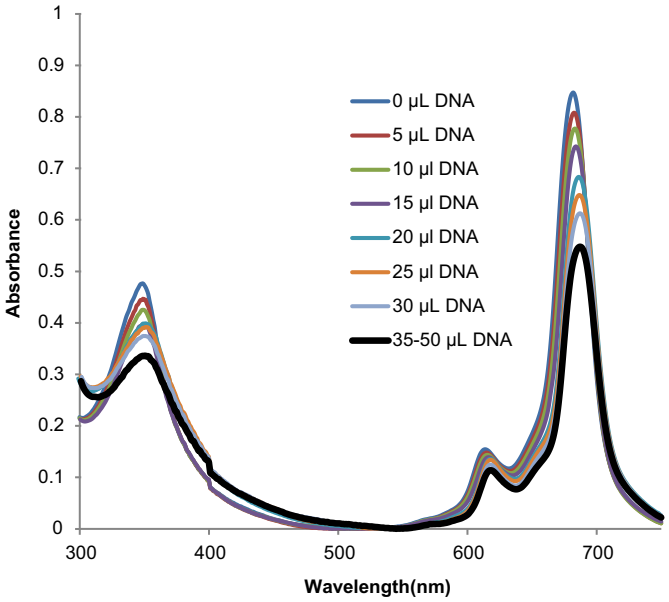

Fig. 7. Electronic spectrum of **4Q** upon increasing amounts of CT-DNA. 10 successive injections (each contained 5 µL 0. 62 mM CT-DNA) were added to 0.035 mM, 1.5 mL buffer solution of **4Q**. Line 1: spectrum of the solution which contained 0.035 mM, 1.5 mL of **4Q**. Line 2–6: The decrease in absorbance continued (Line 2 (5 µL) to line 8 (35 µL)) until a stable dye–Pc complex formed. Line 9 (40 µL)–Line 11 (50 µL) (bold black lines): A stable dye–Pc complex formed when 35 µL (7 × 5) 0.62 mM CT-DNA was added to **4Q**; **Q** band absorbance remained constant after 7th addition.

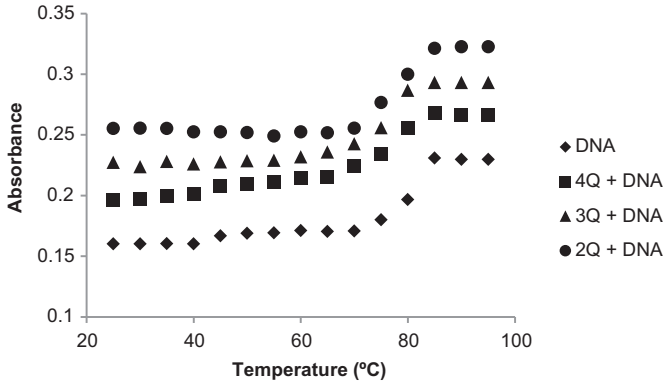

Fig. 8. The thermal denaturation profiles of CT-DNA in the absence and presence of **2Q**, **3Q** and **4Q**. Absorbances are the means of 5 experiments with an average standard deviation of 0.22, 0.20 and 0.17 for **2Q**, **3Q** and **4Q** respectively.

Table 2
Explanation for the samples shown in Lanes 1–6 of gel electrophoresis (agarose 1%) results in Fig. 8, indicating the interaction of **2Q**, **3Q** and **4Q** with DNA.

Lane number	*R* [MPc]/[DNA]
1	0
2	0.25
3	0.50
4	1.00
5	1.50
6	2.00

including; triplet excited-state energy, ability of substituents and solvents to quench the singlet oxygen, the triplet excited-state lifetime and the efficiency of the energy transfer between the triplet excited state and the ground state of oxygen [10,44]. In the presence of quaternary ammonium salts the equilibrium monomer-dimer is shifted to the monomeric form of the complexes, the photocatalytic activity being enhanced in this case (Fig. 4a) [45]. While due to their paramagnetic nature, generally copper and cobalt species deactivate excited states, reducing the excited-state lifetime and preventing photochemical reactions from taking place [46]. Thus, cobalt and copper metallated pcs are not used as photosensitizers. However, after 5 repetition, we concluded that the compound **2Q** can also produce singlet oxygen. Actually, there are well-known examples to this case, including copper octaethyl-benzochlorin [47]. The copper (II)-α-meso-N,N-dimethyl-octaethyl-benzochlorin iminium chloride has a triplet state lifetime which is much too short to allow efficient energy transfer to oxygen with the subsequent generation of singlet oxygen. However, the effectiveness of this compound as a photosensitizing agent for the treatment of urothelial tumors in rats has been clearly demonstrated [47]. Suggestions for this unusual behavior, have pointed to interactions between the cationic iminium group and biomolecules. Such interactions may allow electron-transfer reactions to take place *via* the short-lived excited singlet state and lead to the formation of radicals [48,49]. With the support of published data [47–49], we decided to test the use of these compounds for photocleavage of supercoiled DNA.

The next step was the determination of binding of water soluble **2Q**, **3Q** and **4Q** to CT-DNA. Since mostly biological reactions take place in water, not the compounds (**2**, **3**, **4**) soluble in organic solvents like DMSO but water soluble **2Q**, **3Q** and **4Q** complexes were subjected in this work.

3.3.1. Determination of binding of 2Q, 3Q and 4Q to DNA using UV/Vis titrations

Intercalative binding of small molecules to a DNA helix has been characterized by an appreciable red shift due to the interaction of a DNA π-stack with the π-system of the drug. In general, for a given DNA, intercalation results in large changes in wavelength, whereas groove binding or stacking are reflected by small changes in the UV/Vis spectrum [1,42].

The more increase in aggregation, the more decrease in absorbance of pc derivative and the more interaction with DNA-pc were observed. Thick black lines in Figs. 5 and 6 (lines from 7 to 11 in Figs. 5 and 6 and lines from 9 to 11 in Fig. 7 were running together which means after addition of 25 μL CT-DNA to ***2Q*** and ***3Q***, 35 μL CT-DNA to ***4Q***, the Q band absorbance remained constant) showed the end of titration which means maximum interaction between pcs and DNA occurred. At a final concentration of 0.0344 mM ***2Q*** and ***3Q*** were interacted with DNA while 0.00342 mM ***4Q*** did. According to Fig. 5, **2Q** displayed neither blue nor red shift around Q band (674 nm) region, but a small blue shift at the Soret band (from 330 nm to 328 nm) was observed. In Soret band region of **3Q** (Fig. 6), a shift from 317 nm to 309 nm in Soret region and a red shift from 671 nm to 676 nm indicated that the cationic pcs started to stack at the outside of the DNA stem [1]. Small red shifts at 682 nm (5 nm) and 349 nm (2 nm) for compound **4Q** showed that the occurrence of some form of π stacking interaction [50] further supporting a non-intercalative binding mode with CT-DNA as well as **2Q** and **3Q**. The apparent binding constants (K_a) of **2Q**, **3Q** and **4Q** with DNA were determined as 1.2×10^5 M^{-1}, 1.1×10^5 M^{-1}, 1.08×10^5 M^{-1} for **2Q**, **3Q** and **4Q** respectively. These values are lower than the apparent binding constant normally associated with intercalation ($K_a < 10^6$). They can be attributed to non-intercalative binding mode [1]. However, the decrease in absorption of MPcs' can be assigned to electrostatic attraction between DNA backbone and positive MPcs.

3.3.2. Determination of the change in thermal denaturation profile of DNA

The DNA thermal melting is a measure of the stability of the DNA double helix with temperature an increase in the thermal melting temperature (T_m) indicates an interaction between DNA and the metal complex [42]. In the present case, thermal melting studies were carried out and T_m values were determined by monitoring the absorbance of DNA at 260 nm as a function of temperature. The melting temperature of DNA (T_m) in the presence of a binding molecule or metal can also be used to distinguish between intercalative and external binding modes. Usually, classical intercalation gives rise to higher ΔT_m values than either groove binding or outside stacking [42]. The T_m of DNA in the absence of any added pc was found to be 80 °C ± 0.20, under our experimental conditions. Under the same set of conditions, double helix DNA structure degraded at 82.5 °C ± 0.22, 82.5 °C ± 0.20 and 81.5 °C ± 0.17 in the presence of complexes **2Q**, **3Q** and **4Q** respectively. The observed ΔT_m value of 2.5 °C for **2Q** and **3Q**, 1.5 °C for **4Q** indicates a moderate binding strength between MPcs and CT-DNA. These are consistent with the determined K_a values of 1.2×10^5 M^{-1}, 1.1×10^5 M^{-1}, 1.08×10^5 M^{-1} for **2Q**, **3Q** and **4Q** respectively, further stressing that no classical intercalation took place (Fig. 8).

3.3.3. Determination of binding 2Q, 3Q and 4Q to DNA using gel electrophoresis

The image of the agarose gels of a series of dye/DNA complexes of different ratios (Table 2) are shown in Fig. 9. It was important to see whether CT-DNA would prefer MPcs to SYBR Green I. Thus, the gels were stained by SYBR Green I upon electrophoretic run. It was observed that at low ratios of MPc to DNA, an excess of uncomplexed CT-DNA was present as shown by the migration of the DNA bands. The migration of CT-DNA in the gel was retarded as the ratio of dye to DNA increased, indicating that MPcs were capable of bind to CT-DNA, neutralizing its charges. However, to clarify the difference between **2Q**, **3Q** and **4Q**; the retardation of CT-DNA was

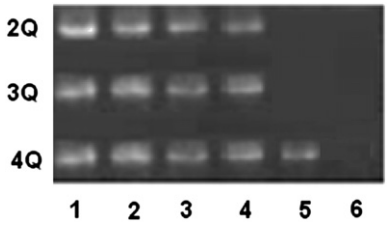

Fig. 9. Gel electrophoresis (1% agarose) results indicating the interaction of DNA with **2Q**, **3Q** and **4Q**. Lane 1 represents control sample which there is no MPc. Lanes 2–6 are the mixtures of CT-DNA with either **2Q**, **3Q** or **4Q** at concentration ratios (R) given in Table 2.

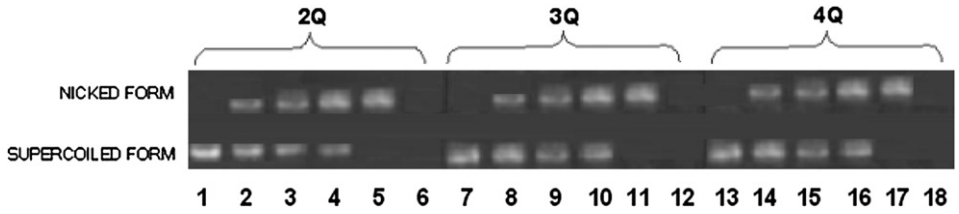

Fig. 10. Agarose (1%) gel electrophoresis pattern for the photocleavage of pBR322 by **2Q**, **3Q** and **4Q**. Reaction mixtures contained 10 μL (0.2 μg) pBR322. Lane 1, 7, 13: pBR322 only. Lane 6, 12, 18: pBR322 + 5 min irradiation ($\lambda > 650$). Lane 5: pBR322 + **2Q**. Lane 11: pBR322 + **3Q**. Lane 17: **4Q** + pBR322. Lane 2: **2Q** + pBR322 + 1 min irradiation. Lane 3: **2Q** + pBR322 + 3 min irradiation. Lane 4: **2Q** + pBR322 + 5 min irradiation. Lane 8: **3Q** + pBR322 + 1 min irradiation. Lane 9: **3Q** + pBR322 + 3 min irradiation. Lane 10: **3Q** + pBR322 + 5 min irradiation, Lane 14: **4Q** + pBR322 + 1 min irradiation. Lane 15: **4Q** + pBR322 + 3 min irradiation. Lane 16: **4Q** + pBR322 + 5 min irradiation.

examined in an increased number of trials. Fig. 9 indicated that **2Q** and **3Q** had slightly more affinity to bind CT-DNA than **4Q** did with expected *R* values of 1.5, 1.5 and 2.0 respectively. These results indicate that the cationic unit of pcs is neutralizing the negative charges of CT-DNA, thereby resulting in the formation of a stable complex. In Fig. 9, complexation of dye-DNA compound was observed clearly; the dye was stuck in the well together with DNA at the top of the gel at high R values (data not shown).

3.4. Determination of photocleavage of plasmid DNA using gel electrophoresis

DNA cleavage was monitored by reaction of supercoiled circular pBR322 (form I) into nicked circular (form II). No DNA scission was observed when the photosensitizer was kept in the dark even though **2Q**, **3Q** and **4Q** were present. When plasmid DNA was subjected to electrophoresis, fast migration was observed for the supercoiled (form I). If scission occurred on one strand (nicking), the supercoils would relax to generate a slower-moving open circular form (form II). A concentration-dependent DNA scission was experienced for all water soluble MPcs (Fig. 10). The binding of Pcs were tested without irradiation at different concentrations (Fig. 9). Thus, the effect of irradiation was evaluated at a constant concentration of reactants with changing irradiation time. As shown in Fig. 10, longer time of irradiation exhibited greater photodamage and formed nicked form DNA. (Lane 2–4 for ***2Q***; 8–10 for ***3Q***; 14–16 for ***4Q***). The binding of pcs to supercoiled DNA was proved with control groups (Lane 5, 11 and 17). There was no effect of irradiation on supercoiled DNA (Lane 6, 12, and 18). These observations correlate well with high singlet oxygen generating efficiency of **2Q**, **3Q** and **4Q**. Therefore, these water soluble pcs have the ability for DNA scission.

4. Conclusion

The main goal of the present work is to address the possible use of water soluble MPcs for biological and biomedical applications. As known, cationic moieties can bind to DNA either intercalatively or electrostatically [51,52] and water soluble nature of drugs enhances the cellular uptake for PDT. Thus we decided to study with a group like seven-membered aza cycle moiety which can be quaternized. Since metals have cytotoxic effects [3,4], copper, cobalt and zinc metals were subjected to test both binding to CT-DNA and producing cytotoxic species. Metals present in pc structure given in Fig. 1 could increase the antitumor effect. Toward this end, metals which are mostly used in biological reactions like copper was incorporated to the pc structure. The binding of all three compounds to CT-DNA was determined by using K binding constants, agarose gel electrophoresis and thermal profiles of DNA. According to results, all new pcs bind to DNA electrostatically. When compared with zinc (**4Q**), binding abilities and singlet oxygen quantum yields of cobalt (**3Q**) and copper (**2Q**) are closer to each other. The most attractive result of our experiments was that the singlet oxygen quantum yields of **2Q** and **3Q** were higher than **4Q** in water (Table 1). It was determined that newly synthesized pcs efficiently exhibit reactive oxygen species as singlet oxygen which can damage cellular components, including DNA, proteins and other macromolecules. This leads to the destruction of cells through apoptosis and/or necrosis. Photocleavage of pBR322 to nicked form II by **2Q**, **3Q** or **4Q** was observed after irradiation (Fig. 10). The longer irradiation time caused greater photodamage on pBR322. In conclusion, we present three water soluble MPcs which bind to CT-DNA electrostatically and have the ability to cleave DNA via Type II mechanism in PDT. Further research on the phototoxicity of these pcs on cell cultures is worthwhile.

Acknowledgments

This work was supported by TUBITAK (110T527) and Research Fund of Istanbul Technical University.

References

[1] Zhanga AM, Huanga J, Wenga X, Lia JX, Rena LG, Songa Z, et al. A water-soluble, octacationic zinc phthalocyanine as molecular probe for nucleic acid secondary structure. Chem Biodiv 2007;4:215–23.
[2] Kaliya OL, Lukyanets EA, Vorozhtsov GN. Catalysis and photocatalysis by phthalocyanines for technology, ecology and medicine. J Porphyr Phthalocya 1999;3:592–610.
[3] Eshkourfu R, Cobeljic B, Vujcic M, Turel I, Pevec A, Sepcic K, et al. Synthesis, characterization, cytotoxic activity and DNA binding properties of the novel dinuclear cobalt(III) complex with the condensation product of 2-acetylpyridine and malonic acid dihydrazide. J Inorg Biochem 2011;105:1196–203.
[4] Galal SA, Hegab KH, Hashem AM, Youssef NS. Synthesis and antitumor activity of novel benzimidazole-5-carboxylic acid derivatives and their transition metal complexes as topoisomerease II inhibitors. Eur J Med Chem 2010;45:5685–91.
[5] Hausman W. Die sensiblisierende wirkund des hematoporphyrins. Biochem J 1911;30:276–316.
[6] Meyer-Betz F. Untersuchungen uber die biologische photodynamische Wirkung des Hematoporphyrins und anderer Derivative des Blu und Galenafarbstoffs. Deutsch Arch. Klin 1913;112:476–503.
[7] Auler H, Banzer G. Untersuchungen über die Rolle der Porphyrine bei Geschwulstkranken Menschen und Tieren. Z Krebsforsh 1942;53:65–8.
[8] Leznoff CC, Lever ABP. Phthalocyanines: properties and applications, vols. 1–4. New York: VCH; 1989–1996.
[9] Mack J, Kobayashi N, Stillman MJ. Magnetic circular dichroism spectroscopy and TD-DFT calculations of metal phthalocyanine anion and cation radical species. J Porphyr Phthalocya 2006;10:1219–37.
[10] Uslan C, Sesalan BŞ, Durmuş M. Synthesis of new water soluble phthalocyanines and investigation of their photochemical, photophysical and biological properties, J Photoch Photobio A, submitted for publication.
[11] Yuksel F, Durmus M, Ahsen V. Photophysical, photochemical and liquid-crystalline properties of novel gallium(III) phthalocyanines. Dyes Pigments 2011;90:191–200.
[12] Sakamoto K, Kato T, Ohno-Okumura E, Watanabe M, Cook MJ. Synthesis of novel cationic amphiphilic phthalocyanine derivatives for next generationphotosensitizer using photodynamic therapy of cancer. Dyes Pigments 2005;64:63–71.

[13] Arvand M, Pourhabib A, Shemshadi R. The potentiometric behavior of polymer-supported metallophthalocyanines used as anion-selective electrodes. Anal Bioanal Chem 2007;387:1033–9.
[14] Chen JC, Chen NS, Huang JF. Derivatizable phthalocyanine with single carboxylgroup: synthesis and purification. Inorg Chem Commun 2006;9:313–5.
[15] Alzeer J, Luedtke NW. pH-mediated fluorescence and g-quadruplex binding of amido phthalocyanines. Biochemistry 2010;49:4339–48.
[16] Nishiyama N, Jang WD, Kataoka K. Supramolecular nanocarriers integrated with dendrimers encapsulating photosensitizers for effective photodynamic therapy and photochemical gene delivery. New J Chem 2007;31:1074–82.
[17] Tamaki Y. Prospects for nanomedicine in treating age-related macular degeneration. Nanomedicine 2009;4:341–52.
[18] Mao JF, Zhang Y, Zhu J, Zhang C, Guo Z. Molecular combo of photodynamic therapeutic agent silicon(IV) phthalocyanine and anticancer drug cisplatin. Chem Commun 2009;8:908–10.
[19] Zheng H, Chen X, Hu MH, Li DH, Xu JG. Near-infrared fluorimetric determination of nucleic acids by shifting the ion-association equilibrium between heptamethylene cyanine and Alcian blue 8GX. Anal Chim Acta 2002;461:235–42.
[20] Spesia MB, Caminos DA, Pons P, Durantini EN. Mechanistic insight of the photodynamic inactivation of *Escherichia coli* by a tetracationic zinc(II) phthalocyanine derivative. Photodiag Photodyn Ther 2009;6:52–61.
[21] Kuznetsova AA, Lukyanets EA, Solovyeva LI, Knorre DG, Fedorova OS. DNA-binding and oxidative properties of cationic phthalocyanines and their dimeric complexes with anionic phthalocyanines covalently linked to oligonucleotides. J Biomol Struct Dyn 2008;26:307–9.
[22] Ben-Hur E, Rosenthal I. Photosensitized inactivation of Chinese hamster cells by phthalocyanines. Photochem Photobiol 1985;42:129–33.
[23] Ali H, van Lier JE. Metal complexes as photo- and radiosensitizers. Chem Rev 1999;99:2379–450.
[24] Atilla D, Saydan N, Durmuş M, Gürek AG, Khanc T, Rück A, et al. Synthesis and photodynamic potential of tetra- andocta-triethyleneoxysulfonyl substituted zinc phthalocyanines. J Photoch Photobio A 2007;186:298–307.
[25] Bonnett R. Photosensitizers of the porphyrin and phthalocyanine series for photodynamic therapy. Chem Soc Rev 1995;24:19–33.
[26] Voge A, Lork E, Sesalan BŞ, Gabel D. N-arylammonio- and N-pyridinium-substituted derivatives of dodecahydro-closo-dodecaborate(2-). J Organomet Chem 2009;694:1698–703.
[27] Sesalan BŞ, Koca A, Gül A. Synthesis and electrochemical properties of porphyrazines with annulated 1,4-dithiaheterocycles. Polyhedron 2003;22:3083–92.
[28] Sesalan BŞ, Koca A, Gül A. Synthesis and characterization of a phthalocyanine–porphyrazine hybrid and its palladium(II) complex. Monat für Chemie 2000;131:1191–5.
[29] Sesalan BŞ, Gül A. Synthesis of novel maleonitrile derivatives. Phosphorus Sulfur Silicon Relat Elem 2003;178:2081–6.
[30] Sesalan BŞ, Koca A, Gül A. Water soluble novel phthalocyanines containing dodeca-amino groups. Dyes Pigments 2008;79:259–64.
[31] Gümüştaş MK, Sesalan BŞ, Atukeren P, Yilmaz B, Gül A. The photodegradation of a zinc phthalocyanine. J Coord Chem 2010;63:4319–31.
[32] Turanlı-Yıldız B, Sezgin T, Çakar ZP, Uslan C, Sesalan BŞ, Gül A. The use of novel photobleachable phthalocyanines to image DNA. Syn Met 2011;161:1720–4.
[33] Farrer Nicola J, Salassa Luca, Peter J. Sadler photoactivated chemotherapy (PACT): the potential of excited-state d-block metals in medicine. Dalton Trans 2009;48:10690–701.
[34] Perrin DD, Armarego WLF. Purification of laboratory chemicals. 2nd edn. Oxford: Pergamon Press; 1989.
[35] Young JG, Onyebuagu W. Synthesis and characterization of di-disubstituted phthalocyanines. J Org Chem 1990;55:2155–9.
[36] Durmus M, Ahsen V. Water-soluble cationic gallium(III) and indium(III) phthalocyanines for photodynamic therapy. J Inorg Biochem 2010;104:297–309.
[37] Brannon JH, Madge D. Picosecond laser photophysics. Group 3A phthalocyanines. J Am Chem Soc 1980;102:62–5.
[38] Seotsanyana-Mokhosi I, Kuznetsova N, Nyokong T. Photochemical studies of tetra-2,3-pyridinoporphyrazines. J Photoch Photobio A 2001;140:215–22.
[39] Kuznetsova N, Gretsova N, Kalmkova E, Makarova E, Dashkevich, Negrimovskii V, et al. Relationship between the photochemical properties and structure of porphyrins and related compounds. Russ J Gen Chem 2000;70:133–40.
[40] Wilkinson F, Helman WP, Ross AB. Quantum yields for the photosensitized formation of the lowest electronically excited singlet state of molecular oxygen in solution. J Phys Chem Ref Data 1993;22:113–262.
[41] Spiller W, Kliesch H, Wöhrle D, Hackbarth S, Roder B, Schnurpfeil G. Singlet oxygen quantum yields of different photosensitizers in polar solvents and micellar solutions. J Porphyr Phthalocya 1998;2:145–58.
[42] Duan W, Zhenxin W, Cook MJ. Synthesis of tetra(trimethylammonio)phthalocyanato zinc tetraiodide, [ZnPc(NMe(3))(4)]I(4), and a spectrometric investigation of its interaction with calf thymus DNA. J Porphyr Phthcya 2009;13:1255–61.
[43] Enkelkamp H, Nolte RJM. Molecular materials based on crown ether functionalized phthalocyanines. J Porphy Phthalocya 2000;4:454–9.
[44] Bıyıklıoglu Z, Durmus M, Kantekin H. Synthesis, photophysical and photochemical properties of quinoline substituted zinc (II) phthalocyanines and their quaternized derivatives. J Photoch Photobio A 2010;211:32–41.
[45] Iliev V, Ileva A. Oxidation and photooxidation of sulfur-containing-compounds in the presence of water soluble phthalocyanine complexes. J Mol Catal A Chem 1995;103:147–53.
[46] Guldi DM, Mody TD, Gerasimchuk NN, Magda D, Sessler JL. Influence of large metal cations on the photophysical properties of texaphyrin, a rigid aromatic chromophore. J Am Chem Soc 2000;122:8289–98.
[47] Selman SH, Hampton JA, Morgan AR, Keck RW, Balkany AD, Skalkos D. Copper benzochlorin, a novel photosensitizer for photodynamic therapy: effects on a transplantable urothelial tumor. Photochem Photobiol 1993;57:681–5.
[48] Garbo GM, Fingar VH, Weiman TJ, Noakes EB, Haydon PS, Cerrito PB, et al. *In vivo* and *in vitro* photodynamic studies with benzochlorin iminium salts delivered by a lipid emulsion. Photochem Photobiol 1998;68:561–8.
[49] Oschner M. Photophysical and photobiological processes in the photodynamic therapy of tumours. J Photoch Photobio B 1997;39:1–18.
[50] Anderson ME, Barrett AGM, Hoffman BM. Binding of octa-plus porphyrazines to DNA. J Inorg Biochem 2000;80:257–60.
[51] Dougherty G. Intercalation of tetracationic metalloporphyrins and related compounds into DNA. J Inorg Biochem 1988;34:95–103.
[52] Cardenas-Jiron GI, Leon-Plata P, Cortes-Arriagada D, Seminario JM. Electrical characteristics of cobalt phthalocyanine complexes adsorbed on graphene. J Phys Chem C 2011;115:16052–62.